This is the peer-reviewed, final accepted version for American Mineralogist, published by the Mineralogical Society of America.
The published version is subject to change. Cite as Authors (Year) Title. American Mineralogist, in press.
DOI: https://doi.org/10.2138/am-2021-7491. http://www.minsocam.org/

Revision 2 – Correction 14 October 2020

For submission to **American Mineralogist**

Plagioclase population dynamics and zoning in response to changes in temperature and pressure

Benjamin J. Andrews

Global Volcanism Program, Smithsonian Institution, Washington, DC 20560

Abstract

Zoned plagioclase crystals are commonly interpreted as proxies for magmatic history, because the mineral occurs in most silicic magmas and has compositional sensitivity to pressure, temperature, and melt composition with slow internal diffusion that preserves zoning. Changes in growth rates and crystal dissolution complicate quantitative relation of time to particular zoning patterns. The numerical model SNGPlag uses Rhyolite MELTS to determine the equilibrium phase assemblage and compositions for a user-defined magma composition, experimentally determined instantaneous nucleation and growth rates, and reasonable dissolution rates to examine plagioclase crystallization and population dynamics through time. SNGPlag tracks the numbers, sizes, morphologies, and compositional zoning of plagioclase crystals through time in response to changes in pressure, temperature, and volume or mass inputs. Results show that significant fractions of time are missing from the crystal record because of effectively zero growth rates, or erased through dissolution; those processes can together remove >>50% of time from the crystal record. Temperature- (or pressure-) cycling alone will not produce substantial

Always consult and cite the final, published document. See http:/www.minsocam.org or GeoscienceWorld

This is the peer-reviewed, final accepted version for American Mineralogist, published by the Mineralogical Society of America.
The published version is subject to change. Cite as Authors (Year) Title. American Mineralogist, in press.
DOI: https://doi.org/10.2138/am-2021-7491. http://www.minsocam.org/

compositional zoning, rather growth of complexly zoned phenocrysts requires the addition of new magma. Comparison of the input pressure-temperature-time series with compositional transects shows the crystal record is biased towards more recent intervals and periods of decreasing temperature (i.e., neither peak temperatures nor intervals of prolonged, cool storage are favored). Crystallization (or dissolution) acts to return magmas to near-equilibrium crystal fractions within 100s of days.

Introduction

Volcanic rocks provide the only record of magmatic processes for all ancient or prehistoric eruptions and at most presently active volcanoes, the exceptions being a relative handful of monitored or instrumented volcanoes. The bulk chemical and isotopic compositions of rock and glass provide an integrative record of fractional crystallization, magma recharge and mixing, and crustal assimilation preceding eruption. Certain mineral phases tend to develop and maintain compositional zoning that records changes in magmatic conditions, providing time-series of magmatic processes.

Plagioclase is used to describe pre-eruptive magmatic processes as it is a generally abundant phenocryst phase common to many volcanic systems. Numerous workers analyze compositional and/or isotopic zoning together with phenocryst textures to interpret changes in pressure and temperature, or magma recharge and mixing (e.g., Gerlach and Grove, 1982; Anderson, 1984; Tsuchiyama, 1985; Singer et al., 1995; Davidson and Tepley, 1997; Tepley et al., 1999; Tepley et al., 2000; Davidson et al., 2001; Costa et al., 2003; Browne et al., 2006; Andrews et al., 2008; Costa et al., 2008; Salisbury et al., 2008; Streck et al., 2008; Waters et al., 2015). U-series geochronometry has been applied to zoned crystals, typically zircons, from some

Always consult and cite the final, published document. See http:/www.minsocam.org or GeoscienceWorld

This is the peer-reviewed, final accepted version for American Mineralogist, published by the Mineralogical Society of America.
The published version is subject to change. Cite as Authors (Year) Title. American Mineralogist, in press.
DOI: https://doi.org/10.2138/am-2021-7491. http://www.minsocam.org/

magmas to constrain the timescales of at least a portion of the histories recorded by individual crystals (Cooper and Reid, 2003; Cooper and Kent, 2014; Budd et al., 2017). Unfortunately, many crystals show evidence of dissolution, thus their records are not complete and the degree to which they are incomplete is largely unknown. This observation, coupled with the variability of growth rates as a function of pressure, temperature, and supersaturation (Hammer and Rutherford, 2002; Mollard, et al., 2012; Befus and Andrews, 2018), complicates quantitative relation of time to particular zoning patterns (Figure 1).

We use a numerical model of crystal nucleation, growth, and dissolution to examine how crystal populations and zoning patterns record time-varying magmatic conditions. The model shows that crystal dissolution is common in magmas with fluctuations in temperature and, to a much lesser extent, pressure (primarily reflecting dissolved water concentration in the melt). Moderate fluctuations in storage conditions can cause some dissolution, and larger excursions in temperature will likely dissolve all small crystals. Consequently, populations of smaller crystals most likely only record events subsequent to the most recent recharge event, whereas larger crystals preserve greater fractions of the total history. Dissolution often removes substantial portions of the crystal record, such that <50% of the total time may be preserved. The relationship between crystal thickness and time is not constant. Because most growth is accommodated during relatively short intervals of cooling following a recharge or heating event, those intervals tend to be overrepresented in the crystals as compared to much longer periods spent at lower temperature.

Background

Always consult and cite the final, published document. See http:/www.minsocam.org or GeoscienceWorld

This is the peer-reviewed, final accepted version for American Mineralogist, published by the Mineralogical Society of America.
The published version is subject to change. Cite as Authors (Year) Title. American Mineralogist, in press.
DOI: https://doi.org/10.2138/am-2021-7491. http://www.minsocam.org/

Phenocrysts form (or dissolve) in response to thermodynamic disequilibrium, e.g., changes in pressure, temperature, oxygen fugacity, and/or composition. Supersaturation results in nucleation and growth of a particular phase, whereas undersaturation results in dissolution (e.g. Ghiorso and Sack, 1995; Gualda et al., 2012; Ghiorso and Gualda, 2015). Nucleation, growth, and dissolution rates are controlled by the degree of disequilibrium, with high supersaturation or undersaturation resulting in faster rates (Donaldson, 1985; Tsuchiyama, 1985; Hammer and Rutherford, 2002; Szramek t al., 2006; Andrews and Gardner, 2010; Brugger and Hammer, 2010; Mollard et al., 2012; Boehnke et al., 2013; Shea and Hammer, 2013; Zhang and Xu, 2016; Befus and Andrews, 2018) with the caveat that high melt viscosities, or other kinetic barriers, can effectively prevent crystallization or dissolution. Both growth and dissolution act to reduce disequilibrium such that crystallization or dissolution rate slows as the magma approaches equilibrium. Growth and dissolution rates describe how fast a single crystal face responds, and the evolution of those rates through time reflects the sum of growth or dissolution across the entire crystal population (Befus and Andrews, 2018; Andrews and Befus, 2020).

Plagioclase feldspar is ubiquitous as a major mineral phase in arc magmas (e.g. Vance, 1965; Nelson and Montana, 1992; Singer et al., 1995; Davidson and Tepley, 1997; Salisbury et al., 2008). The mineral is sensitive to changes in pressure, temperature, and melt composition, with more calcic (anorthitic) compositions occurring in higher temperature, higher pressure (particularly P_{H2O}), and/or more mafic magmas. Numerous experimental studies exploit that compositional dependence to determine pre-eruptive storage conditions (e.g. Rutherford et al., 1985; Gardner et al., 1995; Martel et al., 1999; Andrews and Gardner, 2010; Sosa-Ceballos et al., 2014) and develop various geothermometers and hygrometers (e.g. Housh and Luhr, 1991; Putirka, 2005; Lange et al., 2009; Waters and Lange, 2015). The crystal structure of plagioclase,

Always consult and cite the final, published document. See http:/www.minsocam.org or GeoscienceWorld

This is the peer-reviewed, final accepted version for American Mineralogist, published by the Mineralogical Society of America. The published version is subject to change. Cite as Authors (Year) Title. American Mineralogist, in press. DOI: https://doi.org/10.2138/am-2021-7491. http://www.minsocam.org/

the coupled CaAl-NaSi substitution, and the slow intracrystalline diffusion of those species prevent compositional homogenization, thus compositional zoning is a proxy for the pressure-temperature-compositional history of a given plagioclase. This is in contrast to minerals with no major element sensitivity to those conditions, or those, like olivine, with fast internal diffusion that removes most major element compositional zoning (Shea et al., 2019).

In general, concentrically zoned plagioclase are interpreted to record episodes of increasing and decreasing temperature and/or pressure, as well as changes in magma composition (e.g. Singer et al., 1995; Davidson and Tepley, 1997; Clynne, 1999; Tepley et al., 1999; Tepley et al., 2000; Wallace and Bergantz, 2005; Andrews et al., 2008; Costa et al., 2008; Sosa-Ceballos et al., 2014). Crystal cores record older events than the subsequently formed rims, although sectioning effects biases sampled crystal populations away from cores (Wallace and Bergantz, 2005; Cheng et al., 2017).

Plagioclase zoning patterns are often interpreted to record magma mixing or recharge (e.g. Eichelberger, 1978; Tepley et al., 2000; Humphreys et al., 2006; Andrews et al., 2008; Sosa-Ceballos et al., 2014). Although recharge or mixing can trigger eruption, many of those events do not result in eruption. For example, both El Chichón and Popocateptl show evidence for many more recharge events than eruptions (Espindola et al., 2000; Tepley et al., 2000; Andrews et al., 2008; Sosa-Ceballos et al., 2014).

Non-euhedral growth and crystal dissolution both act to complicate simple "tree-ring" interpretations of zoning. The dependence of growth texture on supersaturation (or undercooling) is explored in detail by Hammer and Rutherford (2002), who demonstrate that euhedral prismatic crystals only nucleate and grow under a limited set of conditions. Sieved plagioclase likely records growth during water-undersaturated decompression (Nelson and Montana, 1992;

Always consult and cite the final, published document. See http:/www.minsocam.org or GeoscienceWorld

Humphreys et al., 2006). Kawamoto (1992) shows that some patchy zoning in plagioclase may record initially skeletal habits, and Shea et al. (2019) have shown that some euhedral olivine crystals form through infilling of initially skeletal growth.

Partial or complete dissolution will occur when a mineral is introduced to a melt in which it is undersaturated (e.g., Donaldson. 1985; Tsuchiyama, 1985; Ghiorso and Sack, 1995; Boehnke et al., 2013; Zhang and Xu, 2016). Dissolution thus removes portions of the crystal record. Many workers have shown that dissolution surfaces are common and often repeated in zoned crystals (e.g. Tepley et al., 1999; Salisbury et al., 2008; Streck et al., 2008). Unfortunately, although differential dissolution between different faces can indicate the minimum amount of dissolution, the absolute amount of dissolution associated with each surface is usually unknown.

Because crystals are the result of time-integrated nucleation, growth, and dissolution processes, the compositional zoning profile of a given crystal can, in principle, be converted into a timeseries if growth and dissolution rates are known or assumed. Many previous experimental studies have described plagioclase nucleation and growth (e.g. Hammer and Rutherford, 2002; Hammer, 2004; Couch et al., 2003; Larsen, 2005; Brugger and Hammer, 2010; Shea and Hammer, 2013; Befus and Andrews, 2018), although most present time-averaged rates. Plagioclase dissolution rates, in contrast, are largely undescribed in the literature, with studies by Tsuchiyama (1985) showing composition-dependent rates, and Donaldson (1985) indicating that dissolution is approximately twice as fast as growth.

Previous researchers apply numerical models to understand and interpret plagioclase zoning patterns, with many of these efforts focused on small amplitude and short length scale oscillatory zoning. Haase et al. (1980) use a composition-dependent growth rate to show that oscillatory zoning can develop over a wide range of parameter space. L'Heureux and Fowler

Always consult and cite the final, published document. See http:/www.minsocam.org or GeoscienceWorld

(1994) show that disequilibrium at the crystal-melt interface drives crystallization, and oscillatory zoning can develop depending on the partition of material into the crystal and the relative growth and diffusion rates. Gorokhova et al. (2013) present a model of plagioclase rim growth during decompression that reproduces compositional zoning observed in samples from Bezymianny. Notably, none of those studies address crystal dissolution, the evolution of populations through time, nor timescales substantially in excess of 10s of days.

Numerical Model of Plagioclase Nucleation, Growth, and Dissolution

We examine plagioclase crystallization and dissolution within an initially 1 m^3 model volume using a modified version of the program SNGPlag (Andrews and Befus, 2020); the new version allows for longer model runs, time-variant temperature and pressure, and crystal dissolution. We briefly describe the original SNGPlag model, before describing the modifications. Following Befus and Andrews (2018) and Andrews and Befus (2020), "supersaturation" describes the disequilibrium of the system, rather than "undercooling," as the former can be readily calculated or measured. Note that in this formulation, a negative supersaturation ("undersaturation") refers to a system with an excess of crystals, i.e. a system in which crystals should dissolve.

SNGPlag Model

Supersaturation Nucleation and Growth of Plagioclase (SNGPlag) is an iterative numerical model that predicts plagioclase sizes and abundances as a function of magma composition, temperature, and decompression path (Andrews and Befus, 2020). At each time, t_i, SNGPlag evaluates the supersaturation, $\Delta\phi$, as the difference between the plagioclase volume

Always consult and cite the final, published document. See http:/www.minsocam.org or GeoscienceWorld

fraction, ϕ, at the previous time step and the equilibrium plagioclase volume fraction, ϕ_{eqb}, as predicted by MELTS (Gualda et al, 2012; Ghiorso and Gualda, 2015) at the specified time-dependent pressure and temperature, $P(t_i)$ and $T(t_i)$. Plagioclase volume fractions ϕ and ϕ_{eqb} are considered on a vesicle-free basis. Nucleation and growth rates, $I(t_i)$ and $J(t_i)$, are defined for the time step as functions of $\Delta\phi$ (Befus and Andrews, 2018). SNGPlag considers the crystals to be rectangular prisms; at each time step, the axes grow by the amount $F\times J(t_i)\times\Delta t$, where F is a factor between 0 and 1 describing the ratio of the axis length to the c-axis length, and Δt is the time step duration. Growth only occurs on crystals or nuclei that exist in the previous step t_{i-1}. Nuclei are added to the model volume in the amount $I(t_i)\times\Delta t$. SNGPlag accounts for volumetric interferences between crystals through an analytical expression that prevents two crystals from occupying the same volume (Andrews and Befus, 2020); potential local variations in crystallization or dissolution rates arising from chemical gradients are not examined. Although growth of real crystals in magmas does not usually result in rectangular prisms, analysis and modeling of realistic textures (swallow tail, hopper, skeletal, etc.; Hammer and Rutherford, 2002) for $>10^9$ crystals is not feasible.

3.2 Modifications to SNGPlag

The new version of SNGPlag allows for variable P-T conditions and longer run times, permitting the study of magmatic processes in the reservoir prior to decompression and eruption. Temperature can follow a prescribed path simulating isothermal (or near isothermal) conditions punctuated by a series of heating or recharge events. Similarly, the system can be isobaric or show fluctuations in pressure as might result from eruption of a portion of the reservoir (Segall,

Always consult and cite the final, published document. See http:/www.minsocam.org or GeoscienceWorld

2016) or from circulation of a parcel of magma through higher and lower pressure regions (Anderson, 1984).

Crystals often reside within magmas for hundreds or thousands of years (e.g. Tepley et al., 1999; Tepley et al., 2000; Cooper and Reid, 2003; Andrews et al., 2008; Cooper and Kent, 2014; Sosa-Ceballos et al., 2014; Budd et al., 2017), but nucleation and growth processes can have timescales of seconds to days (e.g. Gerlach and Grove, 1982; Hammer and Rutherford, 2002; Befus and Andrews, 2018; Andrews and Befus, 2020). The previous version of SNGPlag cannot cover that dynamic range (~8 orders of magnitude). The new version addresses this challenge by calculating changes to the crystal population at fine temporal resolution (600 s), but only recording those changes twice per day (Figure 2). Supplementary Material 1 describes the equations that reduce the temporary population of 120 classes generated at 600 s intervals, each with its own a-, b-, and c- axis dimensions and N_v, into a single characteristic class for each 12 hour period.

The c-axis growth rates used in SNGPlag are from Befus and Andrews (2018). The relative growth rates (J_x) of the a- and b-axes are not constant fractions of the c-axis rate, but instead vary linearly with $\Delta\phi$, from equant or isotropic at $\Delta\phi = 0$, to highly anisotropic at high supersaturations:

$$J_x = (1 + \Delta\phi m_x) J_c \quad \text{Eq. 1}$$

where the subscript x denotes the a- or b-axis, and m_x describes deviation from equant growth; note that the c-axis growth rate does not vary linearly with $\Delta\phi$. The parameter m_x is assumed to be -3 for a and -2 for b; although no systematic examination of m_x as a function of $\Delta\phi$ has been made, experimental studies show that crystal morphologies are more elongate at high degrees of

Always consult and cite the final, published document. See http:/www.minsocam.org or GeoscienceWorld

disequilibrium (e.g. Hammer and Rutherford, 2002; Szramek et al., 2006) and the chosen m_x values produce reasonable crystal shapes. We use the expression

$$Sn_i = \sum N_i \left({L_{ai}}^2 + {L_{bi}}^2 + {L_{ci}}^2\right)^{1/3} \Big/ \sum N_i \qquad \text{Eq. 2}$$

to obtain the characteristic crystal size Sn at each time i. The anorthite content (An) at time i is determined using MELTS as a function of pressure and temperature, resulting in a-, b-, and c-axis growth patterns and compositions within each crystal.

Crystal dissolution is an important and frequent process within many magmatic systems (Tepley et al., 1999; Tepley et al., 2000; Andrews et al., 2008; Salisbury et al., 2008; Streck et al., 2008; Sosa-Ceballos et al., 2014). The stable composition of plagioclase varies with pressure and temperature (e.g. Rutherford et al. 1985; Putirka, 2005; Lange et al., 2009; Andrews and Gardner, 2010; Sosa-Ceballos et al., 2014; Waters and Lange, 2015; Waters et al., 2015), such that unless the system becomes superliquidus with respect to plagioclase, only certain compositions will dissolve (Tsuchiyama, 1985). We assume that dissolution rate is a function of undersaturation ($\Delta\phi<0$), thus dissolution is faster in highly undersaturated systems. The dissolution rate follows the same functional form as the c-axis growth rate, but with a two-fold increase in magnitude; e.g., if $\Delta\phi=0.1$ results in a growth rate of ~0.2 μm/h, then $\Delta\phi=-0.1$ results in a dissolution rate of ~0.4 μm/h. Experimental work by Tsuchiyama (1985) and Donaldson (1985) suggests this assumption of faster dissolution rates as compared to growth rates is reasonable. Recent papers combining experimental measurements of diffusion and zircon saturation (Boehnke et al., 2013; Zhang and Xu, 2016) show that zircon dissolution rate rapidly increases as the zircon liquidus is exceeded; applying their general findings to plagioclase, the

Always consult and cite the final, published document. See http:/www.minsocam.org or GeoscienceWorld

dissolution rates of unstable plagioclase compositions should increase with the magnitude of undersaturation. We assume dissolution rates are isotropic. Finally, to account for the potential stability of relatively higher An compositions of plagioclase (Tsuchiyama, 1985), SNGPlag only dissolves plagioclase with An less than the equilibrium value calculated by MELTS for the pressure and temperature at that time step.

Together, the $\Delta\phi$-dependent anisotropic growth rates and $\Delta\phi$- and An-dependent dissolution rates allow SNGPlag to grow complexly zoned crystals. A P-T trajectory resulting in increasing $\Delta\phi$ and decreasing An produces a concentrically zoned crystal with a higher An core and lower An rim. If that crystal undergoes a dissolution event followed by renewed crystallization, the concentric zoning will be truncated with greater fractions of the a- and b-axes dissolved compared to the c-axis (Figure 3). Repeated episodes of dissolution and crystallization can produce crystals with oscillatory zoning in the c-axis and effectively monotonic zoning in the a- and/or b-axes (Figure 3).

The modified model allows a change in system volume during recharge events. As temperature increases, volume can increase by a specified fraction of crystal-free melt with an identical bulk composition as the original magma, decreasing total crystallinity. For example, an increase of 0.1 decreases crystallinity by a factor of ~0.09 (=1/(1+0.1)).

SNGPlag assumes that the other crystal phases are in instant equilibrium. The model does not account for changes in melt composition through time. Although tracking compositional changes during crystallization is trivial, calculating those changes during dissolution of compositionally zoned anisotropic crystals is not feasible.

We use the nucleation and growth rates presented in Befus and Andrews (2018) as these are the only published instantaneous rates. All other published values are presented as time-

Always consult and cite the final, published document. See http:/www.minsocam.org or GeoscienceWorld

averaged rates, generally as functions of initial undercooling (Hammer and Rutherford, 2002; Couch et al., 2003; Larsen, 2005; Brugger and Hammer, 2010; Shea and Hammer, 2013). Use of time-averaged rates in an instantaneous model results in either impossibly large crystals and high crystallinities (applied to model durations of years or centuries such rates produce m-scale crystals in mm-scale volumes of magma), or implausibly low crystallinities (when converted to time-variant rates). The Results section presents the effects of variation in nucleation, growth and dissolution rates on model outputs.

The terms “antecryst,” “phenocryst,” and “microlite” follow the definitions used in Andrews and Befus (2020). The initial antecryst volume does not affect the system equilibrium, although subsequent crystallization on antecrysts will affect equilibrium. Phenocrysts are crystals present at the start of the run whose initial volume contributes towards equilibrium. Microlites are defined as those crystals that nucleate and grow during the course of the simulation.

Model results

We present three suites of model runs using an El Chichón trachyandesite bulk composition (Macias et al., 2003; Andrews et al., 2008; Table 1). First, we examine the system response to step-like changes in temperature to establish timescales over which a magma returns to equilibrium during 2-year model runs. These simulations act as simplified perturbation analyses of a more complex natural system and are discussed in the context of model sensitivity to nucleation, growth, and dissolution rates. Second, we consider 2-year simulations with repeated heating-cooling or decompression-pressurization cycles to understand how crystal populations survive intervals of crystallization and dissolution. Finally, we parameterize model

Always consult and cite the final, published document. See http:/www.minsocam.org or GeoscienceWorld

This is the peer-reviewed, final accepted version for American Mineralogist, published by the Mineralogical Society of America.
The published version is subject to change. Cite as Authors (Year) Title. American Mineralogist, in press.
DOI: https://doi.org/10.2138/am-2021-7491. http://www.minsocam.org/

results and extend a simplified version of the model to a ~5300-year interval to study what fractions of magmatic history are preserved within a single crystal.

Timescales of equilibration and model sensitivity

Model runs with step-like changes in temperature rapidly increase the disequilibrium magnitude ($|\Delta\phi|$) and show how quickly the magma returns to or approaches equilibrium. After an initial dwell time of 182.5 days (0.5 years) at T_o, temperature changes to T_f over 1 day, and then holds at T_f for the remainder of the 2-year run; simulations with $T_f > T_o$ record negative values of $\Delta\phi$, resulting in dissolution, whereas runs with $T_f < T_o$ show positive excursions in $\Delta\phi$, and thus crystal nucleation and growth. These runs have no volume addition.

Figure 4A shows variation in $\Delta\phi$ with respect to time, and thus how quickly the systems equilibrate. The rate at which $|\Delta\phi|$ decreases is proportional to $|\Delta\phi|$. Because the experimentally determined nucleation and growth rates are very low for $\Delta\phi < 0.04$, reduction of $|\Delta\phi|$ to $<<0.04$ occurs slowly, with an asymptotic approach to $\Delta\phi=0$. Larger initial excursions in $\Delta\phi$ require longer recovery times. Although the instantaneous dissolution rate is at least twice as fast as the growth rate for undersaturation and supersaturations with the same magnitude, system equilibration rates differ by less than a factor of 2, likely because dissolution acts on a decreasing number of crystals with decreasing size, whereas growth acts on an increasing number of ever larger crystals.

To examine SNGPlag sensitivity to nucleation, growth, and dissolution rates, we vary the magnitudes of those rates from 25 times less (i.e. roughly comparable to rates from Hammer and Rutherford, 2002) to 5 times greater, while maintaining the same functional form as in Befus and Andrews (2018). Figure 4B shows that slower rates, varied individually or jointly, result in

Always consult and cite the final, published document. See http:/www.minsocam.org or GeoscienceWorld

slower equilibration. Faster rates result in faster equilibration, with the decrease in response time approximately proportional to the increase in rate. Changes in nucleation and growth rate both affect crystallization responses during intervals of supersaturation. Not surprisingly, the dissolution response during heating is most sensitive to changes in dissolution rate, with minor sensitivity to nucleation rate, as nucleation affects the initial crystal population.

Nucleation, growth, and dissolution rates also affect the fidelity with which individual crystals record magmatic history. Supplementary Material 2 shows zoning pattern sensitivity to variation in those rates from 25 times less to 10 times greater than those from Befus and Andrews (2018). Elevated growth rates produce large crystals recording large time fractions (>70% in the test scenario) when nucleation rate is low, with changes in dissolution rate only causing minor differences in the crystal record. High nucleation rates result in low recorded time fractions (~10%) even at high growth rates. The recorded time fraction varies inversely with covariation in nucleation, growth, and dissolution rates such that for elevated or nominal values, the crystals record ~10% of the scenario, but preserved time fraction increases to ~18 and ~37% as the rates decrease to 0.1 and 0.04 times the nominal values, respectively. Low growth rates produce small crystals; complete dissolution of such crystals is common during heating or recharge events except when nucleation and dissolution rates are both reduced.

The time series for different magnitude heating or cooling events collapse onto single dissolution or crystallization trajectories. Time series with lower $|\Delta\phi|$ can be overlain onto the highest $|\Delta\phi|$ series by introducing a lag in the time indices of the lower $|\Delta\phi|$ series. Crystallinity (expressed as $\Delta\phi$) does not vary exponentially with time nor follow a “half-life” return to equilibrium, but instead $|\Delta\phi|$ decreases approximately linearly as a function of $|\Delta\phi|$ in log-log space. These patterns indicate that the maximum disequilibrium experienced by a system

Always consult and cite the final, published document. See http:/www.minsocam.org or GeoscienceWorld

DOI: https://doi.org/10.2138/am-2021-7491. http://www.minsocam.org/

controls the time over which that system approaches equilibrium, and that $\Delta\phi$ can predict the instantaneous rate of system crystallization or dissolution when the nucleation, growth, and dissolution rates are known. Although this predicted response is not as precise as the full model, it can inform longer duration models of crystallization.

Repeated oscillations in temperature and/or pressure

Thermal cycling

We examine repeated cycles of magma heating and cooling, conceptually analogous to the thermal effects of recharge on a host magma. We begin with an initial temperature T_o then increase temperature to T_f, before returning to T_o. The T-t series follows a Gaussian path described by the error function; heating of the magma in this scenario occurs ~3 times more rapidly than cooling such that a 60-day total duration heating event achieves a maximum temperature after 15 days. We present four runs, each with three heating events. The initial equilibrium crystal fraction plagioclase for all scenarios is 0.413, and the runs begin with ϕ_{plag}=0.207 comprising equal fractions of 200, 150, 100, and 75 μm cubic crystals. Supplementary Material 3 describes presentation of 3D crystal shapes.

Figure 5 shows results from a 2-year model run at T_o=800 °C with 60-day 100°C heating events with no volume addition, occurring at 6, 12, and 18 months. During each event, crystallinity decreases during heating and increases during cooling. The crystal population changes through the model run, with maximum numbers present immediately before initiation of each recharge event (and at the end of the run), and minimum numbers present during high temperature intervals. Most of the crystals that form do not survive subsequent recharge events, the population always comprises a small number of phenocrysts and a small subset of early-

Always consult and cite the final, published document. See http:/www.minsocam.org or GeoscienceWorld

nucleated crystals, with a subordinate number that nucleate and dissolve until the final thermal maximum is achieved (Figure 5c and 5d). As a consequence, the characteristic crystal dimensions (Figure 5e) are dominated by the early-formed crystals with only minor excursions reflecting the nucleation and dissolution of new crystals; the crystal size Sn, however, shows step changes as crystals nucleate and dissolve. The characteristic shape for all crystals (Figure 5f) gradually elongates through time, reflecting effectively isotropic dissolution followed by non-isotropic (e.g., c>b>a axis) growth; the shape of newly grown crystals is more elongate and oscillates over the same range through each cycle.

Figure 6 shows a run with identical conditions as presented in Figure 5, but with volume addition of 0.25 during each heating event. The additional volume decreases the plagioclase volume fraction during heating, reducing undersaturation magnitude. The slower dissolution rates and reduced total amount of dissolution allow survival of more crystals, with nearly all crystals nucleated prior to the first heating event, and a portion of those nucleated after the first thermal maximum, surviving to the end of the model run (Figure 6c). The preservation of a more diverse crystal population also damps the step-like variations in Sn (Figure 6e). Characteristic crystal shapes lengthen with time (Figure 6f).

Crystal dissolution during and growth following heating events are inversely and directly proportional to volume fraction input, respectively (Figure 7). Volume addition makes zones larger, and reduces their subsequent dissolution. Increased volume during heating events also affects crystal compositional zoning. Figure 8 shows a-, b-, and c-axis transects of An and the times that are recorded by a crystal nucleated at day 1 for the scenarios shown in Figure 5 and 6. Although the c-axis profiles for both crystals show 3 peaks in An, the scenario with volume addition preserves 2 peaks in the a- and b-axes. Volume addition preserves the a- and b-axis

Always consult and cite the final, published document. See http:/www.minsocam.org or GeoscienceWorld

zones grown following the first heating event – a fraction of crystal completely dissolved during the scenario with no volume addition.

Not all recharge events should be the same temperature, nor affect all regions of the host magma with the same magnitude and duration of temperature excursion, therefore we conduct 2-year model runs with 120-day recharge events of increasing and decreasing thermal magnitudes (Figure 9). For these simulations, volume addition during each recharge event is 0.1. In systems with increasing temperatures, no crystals nucleated following one recharge event survive the next recharge event. In contrast, the run with decreasing magnitude heating events preserves a large number of crystals; all crystals formed above 200°C during cooling following the first thermal maximum survive until the end of the run, as do all formed above 150°C during cooling following the second thermal maximum. The characteristic sizes and shapes evolve differently for the two scenarios. In the increasing series, Sn evolves strong peaks during the heating events, reflecting dissolution of all but the largest crystals, whereas in the decreasing series Sn remains low after the first event because some small crystals survive each heating event. Similarly, the increasing series shows more variation in characteristic shape and finishes with slightly more elongate morphology.

Pressure cycling

Pressure within a magma reservoir may drop during eruption (e.g. Anderson, 1984; DeGruyter and Huber, 2014; Segall, 2016; Townsend et al., 2019). The decompression magnitude and the timescale over which pressure returns to its initial value are functions of numerous factors including magma and host rock compressibility and the ratio of erupted to reservoir volume (Huppert and Woods, 2002; DeGruyter and Huber, 2014; Segall, 2016;

Always consult and cite the final, published document. See http:/www.minsocam.org or GeoscienceWorld

This is the peer-reviewed, final accepted version for American Mineralogist, published by the Mineralogical Society of America.
The published version is subject to change. Cite as Authors (Year) Title. American Mineralogist, in press.
DOI: https://doi.org/10.2138/am-2021-7491. http://www.minsocam.org/

Townsend et al., 2019). We consider comparatively rapid decompression events as generated by eruptions that are followed by more gradual return to the initial pressure. The P-t path follows the same functional form as the recharge events, with the minimum pressure achieved at 25% of the total cycle duration. During each decompression-pressurization cycle, no volume is added to the system. Note that a decompression event is equivalent to a cooling event within SNGPlag, as both result in an initial increase then decrease in $\Delta\phi$.

Figure 10 shows the P-t path for a sequence of three decompressions from 100 to 50 MPa at 800 °C with event durations of 120 days. These decompressions are of larger magnitude than might be expected during most natural eruptive cycles, but have $|\Delta\phi|$ roughly comparable to cooling from 800 to ~750°C; smaller, more geologically plausible decompressions manifest virtually no crystallization record in SNGPlag. Pressure cycling begins with a positive change in $\Delta\phi$, resulting in nucleation and growth. The system remains plagioclase-supersaturated during repressurization ($\Delta\phi$ remains positive), thus although nucleation and growth rates decrease, the system never dissolves crystals. This lack of dissolution results from pressure cycles with durations comparable to or less than the timescales required for equilibration, and decompression inducing small amplitude changes in $\Delta\phi$ (< ~0.03). Larger magnitude or longer duration pressure cycles might result in dissolution during the later stages of repressurization.

Modelling longer run durations

The previously discussed runs had 2-year durations, with one 10-year simulation used to examine how systems approach equilibrium over a longer time. Magmatic processes, however, often occur over much longer intervals, and individual crystals can reside in magmas for thousands of years (Cooper and Reid, 2003; Andrews et al., 2008; Cooper and Kent, 2014; Sosa-

Always consult and cite the final, published document. See http:/www.minsocam.org or GeoscienceWorld

DOI: https://doi.org/10.2138/am-2021-7491. http://www.minsocam.org/

Ceballos et al., 2014; Budd et al., 2017). We use the equilibration timescales determined above to develop a simplified model of plagioclase $\Delta\phi$ as a function of P-T-t path. That $\Delta\phi$ timeseries allows calculation of the growth, dissolution, and compositional history of a single crystal over a geologically interesting interval. We describe that simplified model, validate it against a 5-year run of SNGPlag to ensure that it can recover results of the full model, and then use it to examine a hypothetical ~5300-year P-T-t series.

At a constant equilibrium crystallinity ϕ_{EQB}, the rate at which $\Delta\phi$ changes ($\Delta\phi/dt$) describes the crystallization rate of that system. The equilibration timeseries discussed previously and displayed in Figure 4 show $\Delta\phi/dt$ is proportional to $\Delta\phi$. If plagioclase crystallinity (ϕ) is known, then $\Delta\phi$ can be calculated as $\Delta\phi=\phi_{EQB}-\phi$, which can determine $\Delta\phi/dt$ at that time. That rate describes the amount of crystallization (or dissolution) during the next time step. At that new time t_i, the difference between ϕ and ϕ_{EQB} determines $\Delta\phi$, and the model thus proceeds iteratively, as shown in the expression:

$$\phi_i = \phi_{i-1} + \left({}^{\Delta\phi}/_{dt}\right)_{i-1} \Delta t \qquad \text{Eq. 3}$$

Although this approach may accumulate uncertainty, the timescales required for equilibration are 100s of days, thus intervals spent at constant conditions for more than one year prevent forward propagation of those errors.

We compare this approximation to a 5-year run of SNGPlag. The runs have a series of convolved temperature and pressure changes (Figure 11), allowing examination of plagioclase population dynamics over a range of temperature, pressure, and time scales. Comparison of $\Delta\phi$

Always consult and cite the final, published document. See http:/www.minsocam.org or GeoscienceWorld

between the full and simplified runs shows good agreement (Figure 11) indicating the parameterized version can recover results of the full model.

We now consider a magma over ~5300 years with a randomly generated recharge and eruption history. Series of recharge events occur every 200 years (Figure 12). Each series can last from 10-100 years, with up to 5 events per decade. Those events have 50-150 °C magnitudes, durations of 0.25-10 years, volume fraction additions of 0-0.5, and can be superimposed upon one another. Each recharge series can also have an eruption, i.e. an interval of 10-25 MPa decompression over up to 7 days, with the system returning to its initial pressure (100 MPa) over 0.25-10 years. The initial pressure is at the lower bound of likely storage pressures for the Chichón trachyandesite (Macias et al., 2003) or other intermediate arc magmas, but is chosen because allows for a larger thermal range of plagioclase stability and composition than higher pressures. Runs at higher pressures show a systematic decrease in the fraction of time preserved in crystals as the same temperature excursions induce greater magnitude $|\Delta\phi|$ and potentially more time spent at or above the plagioclase liquidus. The modeled interval contains a total of 454 recharge events and 12 decompressions or eruptions occurring in 26 groups. These values do not mimic any specific volcano or series of eruptions, but rather examine a geologically reasonable family of recharge and eruption scenarios (Andrews and Manga, 2014; Cooper and Kent, 2014; Sosa-Ceballos et al., 2014; Segall, 2016).

Figure 13 shows the final compositional zoning profile for the P-T-t series. Supplementary Material 4 shows an animation of the compositionally zoned crystal, illustrating growth, dissolution, and compositional profiles through time. In runs with zero or low volume additions during heating events, the system repeatedly crystallizes and dissolves variations of the same zone, thus no net growth occurs (Supplementary Material 5). Each heating-cooling episode

Always consult and cite the final, published document. See http:/www.minsocam.org or GeoscienceWorld

DOI: https://doi.org/10.2138/am-2021-7491. http://www.minsocam.org/

results in possible dissolution followed by crystallization of initially higher An plagioclase followed by decreasing An plagioclase. Moving outward from the core, approximately 20 distinct An peaks with step-like increases of >10 mol.% are preserved in the record. This number is lower than the >400 total recharge events in the temperature timeseries (Figure 12). The lower number of recorded events is expected as some of the recharge events are superimposed on one another, resulting in effectively singular events, and because dissolution removes portions of the crystal record. In addition, the crystal completely dissolves twice during the first 2000 years (Figure 13).

The ~5300-year magmatic history is not uniformly sampled by the crystal (Figure 13). The more complete zoning patterns preserved in the c- versus a- and b-axes show that large fractions of the crystal record are missing. Not only are intervals of dissolution missing from the crystal, but its record is dominated by intervals of high supersaturation during which faster growth occurs. This has the effect of undersampling higher- and lower-temperature intervals (those with the highest and lowest An compositions). A histogram of An composition indicates that the range of P-T conditions recorded by the crystal approximates the range of conditions experienced by the magma, but its distribution is not proportional to the time spent at those conditions (Figure 13).

Discussion

SNGPlag predicts how plagioclase populations evolve in response to changes in temperature and pressure. Heating or pressurization result in dissolution, whereas cooling or decompression result in nucleation and growth. More anorthitic plagioclase forms at elevated temperature and pressures, thus an individual recharge event is likely recorded as a step-like

Always consult and cite the final, published document. See http:/www.minsocam.org or GeoscienceWorld

DOI: https://doi.org/10.2138/am-2021-7491. http://www.minsocam.org/

increase in An, followed by a more gradual decline. Because SNGPlag conditions dissolution on An, a high-An zone can shield inboard regions from dissolution. The net results of these processes are that smaller, more albitic plagioclase dissolve more easily than larger plagioclase with more anorthitic zones, and that high temperature excursions often dissolve crystals (or zones) formed during preceding cooler intervals including recharge events of smaller thermal magnitude.

Large crystals survive for longer intervals and effectively grow at the expense of smaller crystals. This process is not Ostwald ripening, but the interplay of outward growth and inward dissolution rates of crystal faces. Growth and dissolution have units of distance per time, as these processes occur through the incremental addition or removal of atoms from crystal faces; defining these rates with units of volume (or volume fraction) per time presupposes a crystal number density and size distribution. The same growth rate applied to large and small crystals crystallizes much more material onto the former, more rapidly reducing supersaturation and retarding additional crystallization. Larger crystals are more likely to contain high-An zones that shield albitic interiors. Consequently, smaller crystals completely dissolve more readily than large crystals, and repeated dissolution-crystallization cycles can increase the size of surviving crystals.

Net growth requires mass addition

If the modeled system has no additions of mass (or volume), then those crystals (or zones) formed during the initial crystallization event and/or some final temperature decrease are most likely to be preserved; crystals formed during earlier, lower temperature intervals will be dissolved. Oscillatory zoning with compositional range >10 mol.% An (and perhaps less) is

Always consult and cite the final, published document. See http:/www.minsocam.org or GeoscienceWorld

unlikely to form only through cycling of temperature and/or pressure, but also requires mass addition.

The addition of mass to the system during recharge events has the effect of reducing total crystallinity, thereby reducing the undersaturation magnitude . Although dissolution can still occur during an episode of heating, reduction of system crystallinity allows the magma to crystallize a larger final fraction than initially dissolved (i.e., 9 vol.% dissolves, but 10 vol.% crystallizes). Without mass addition, the same zones repeatedly grow and dissolve, thus oscillatory or complex zoning cannot develop.

This required mass addition does not mean that the total magma reservoir increases in volume by, e.g., 10%, only that the volume interacting with the crystal(s) of interest increases. The new mass need not be directly from the recharging magma, but could be remobilized host magma. This further highlights how two crystals might record the same event differently (Andrews et al., 2008; Sosa-Ceballos et al., 2014): a crystal near enough to the recharging magma to encounter the added mass would partly dissolve before growing a larger new zone and increasing in size, whereas a more distal crystal might dissolve before growing a roughly equivalent new zone resulting in no change in crystal size. Analysis of trace element or isotopic zoning, in tandem with An zoning, can identify whether the added mass is remobilized from the host or is new magma entering the system (Tepley et al., 1999; Tepley et al., 2000; Andrews et al., 2008).

Application to natural systems

This paper does not precisely model a specific natural system. Although the presented simulations use El Chichón trachyandesite compositions, the Chichón magma system has

Always consult and cite the final, published document. See http:/www.minsocam.org or GeoscienceWorld

processes and characteristics beyond consideration of this model. Further, SNGPlag assumes dissolution rates and axis-dependent growth rates that are reasonable but not experimentally verified for Chichón. Despite those simplifications, the model offers insights into natural magma dynamics, and the parameterized model can be applied to an arbitrary magma composition by using MELTS to determine the plagioclase volume fraction and composition as functions of pressure and temperature.

First, because plagioclase growth and dissolution rates are very low at small $|\Delta\phi|$, growth and dissolution are not sensitive to small changes in pressure, temperature, or composition. Whereas large excursions in disequilibrium will return to $|\Delta\phi|<0.05$ in 100s of days, reduction in $|\Delta\phi|$ to <0.02 requires times in excess of 150 years; even if that second timescale is too long, the pattern of asymptotic equilibration holds, and magmas should show limited response to small changes in $\Delta\phi$. Crystallization (or dissolution) will maintain equilibrium, or a state near equilibrium, with any changes in intensive parameters occurring over timescales >100s of days.

Second, dissolution and changing growth rates result in the absence of substantial amounts of time from most crystal records. It is not unreasonable for 50% of a crystal to form during 10% of its history, and 75% of its total history to be removed by dissolution. This observation is similar to the “cold storage” hypothesis of Cooper and Kent (2014), where magmas spend substantial fractions of time in a cool, rheologically locked, uneruptible state, but with the extension that many intervals are entirely removed from individual crystals. Our results show that the plagioclase record is biased against high-temperature intervals, although more limited information describing high-temperature thermal state may be preserved by diffusion profiles within crystals, such as duration and magnitude of heating. Future work, involving a large number of model runs with P-T-t paths informed by other petrologic observations and

Always consult and cite the final, published document. See http:/www.minsocam.org or GeoscienceWorld

numerical models (e.g. Andrews et al., 2008; DeGruyter and Huber, 2014; Sosa-Ceballos et al., 2014; Townsend et al., 2019) could quantify bias in the crystal record as a function of recharge volumes, and recharge and eruption frequencies.

Third, the c-axis preserves a more complete record than other crystallographic axes. This is true because the faster growing axis stretches zoning patterns compared to the a- and b-axes, and also because dissolution completely removes zones from faces normal to the a- and b-axes. Previous workers have noted that the c-axis provides the best opportunity to correlate crystals (e.g., Wallace and Bergantz, 2002, 2004, 2005), but observational artifacts and magmatic processes complicate correlation (Wallace and Bergantz, 2005; Andrews et al., 2008; Cheng et al., 2017). Robust correlations likely require analysis of large numbers of crystals from the outside in, and matching both the shape and magnitude of zones because they record separate aspects of magmatic history: the change in An provides an indication of the absolute change in temperature (or melt composition), whereas the shape of a zone records $\Delta\phi$ through time.

Implications

SNGPlag suggests the plagioclase record is biased against higher and lower An compositions and towards more recent time intervals. Although the plagioclase compositional range reflects the pressure-temperature-composition range experienced by the magma, the fraction of high- to low-An zones does not record the relative time spent at those conditions. Further, the smallest crystals likely only record time since the most recent dissolution event.

Substantial intervals of time are not recorded by phenocrysts. Depending upon the amount of mass addition that occurs in close proximity to a crystal during recharge or heating

Always consult and cite the final, published document. See http:/www.minsocam.org or GeoscienceWorld

events, dissolution can erase and slow growth rates can compress large fractions of a crystal's history. Together those processes can remove more than 50% of time from a crystal record.

Complex compositional zoning in plagioclase requires mass addition as well as heating. Significant heating with little or no mass addition results in substantial dissolution and obliteration of the crystal record. The common occurrence of complex compositional zoning indicates that most heating events experienced by individual crystals, or at least those preserved in crystals, are accompanied by new melt.

Mixed crystal populations are ubiquitous in arc andesites and dacites. The compositional range in any crystal records the pressure-temperature-composition-time (P-T-X-t) conditions that crystal experienced; but that history may not be representative of the magma in general. Obtaining a unified P-T-X-t history of a magma requires reconciling disparate records of many crystals. The complexity in resolving those histories should indicate the timescales and length scales of magmatic processes: large, prolonged events affecting the entire magma body should be recorded more uniformly than small events only recorded by crystals in close physical proximity to the disturbance.

Plagioclase populations approach equilibrium with magma intensive parameters over timescales of 100s of days, thus those populations effectively maintain textural (and compositional) equilibrium during processes operating over timescales longer than a year (e.g., gradual heating or cooling). The lag between the onset of some rapid process and the crystallization response of the magma(s) is thus shorter than 100s of days. Consequently, the interval during which neither a hot intruding magma nor cool host magma are sufficiently crystallized to be rheologically locked is on the order of months, thus fluid mixing of compositionally and/or thermally distinct magmas must occur over similar timescales.

Always consult and cite the final, published document. See http:/www.minsocam.org or GeoscienceWorld

Acknowledgements

The SNGPlag model benefited from helpful discussions with KS Befus, MS Ghiorso, and G Sosa-Ceballos. C Huber and A Kent provided thoughtful reviews that improved this manuscript.

This is the peer-reviewed, final accepted version for American Mineralogist, published by the Mineralogical Society of America.
The published version is subject to change. Cite as Authors (Year) Title. American Mineralogist, in press.
DOI: https://doi.org/10.2138/am-2021-7491. http://www.minsocam.org/

References

Anderson, AT (1984) Probable relations between plagioclase zoning and magma dynamics, Fuego Volcano, Guatemala. American Mineralogist, 69:660-676

Andrews BJ, Befus KS (2020) Supersaturation Nucleation and Growth of Plagioclase: a numerical model of decompression induced crystallization. Contributions to Mineralogy and Petrology, 175: 23 https://doi.org/10.1007/s00410-020-1660-9

Andrews BJ, Gardner JE (2010) Effects of caldera collapse on conduit dimensions and magma decompression rate: an example from the 1800 14C yr BP eruption of Ksudach Volcano, Kamchatka, Russia. Journal of Volcanology and Geothermal Research, 198:205-216.

Andrews BJ, Gardner JE, Housh TB (2008) Repeated recharge, assimilation, and hybridization in magmas erupted from El Chichón as recorded by plagioclase and amphibole phenocrysts. Journal of Volcanology and Geothermal Research,175:415-426

Andrews BJ, Manga M (2014) Thermal and rheological controls on the formation of mafic enclaves or banded pumice. Contributions to Mineralogy and Petrology,167:961

Befus KS, Andrews BJ (2018) Crystal nucleation and growth produced by continuous decompression of Pinatubo magma. Contributions to Mineralogy and Petrology,173:92. doi.org/10.1007/s00410-018-1519-5

Boehnke P, Watson EB, Trail D, Harrison TM, Schmitt AK (2013) Zircon saturation revisited. Chemical Geology, 351:324-334

Browne BL, Eichelberger JC, Patino LC, Vogel TA, Uto K, Hoshizumi H (2006) Magma mingling as indicated by texture and Sr/Ba ratios of plagioclase phenocrysts from Unzen volcano, SW Japan. Journal of Volcanology and Geothermal Research, 154:103-116

Always consult and cite the final, published document. See http:/www.minsocam.org or GeoscienceWorld

This is the peer-reviewed, final accepted version for American Mineralogist, published by the Mineralogical Society of America.
The published version is subject to change. Cite as Authors (Year) Title. American Mineralogist, in press.
DOI: https://doi.org/10.2138/am-2021-7491. http://www.minsocam.org/

Brugger CR, Hammer JE (2010) Crystal size distribution analysis of plagioclase in experimentally decompressed hydrous rhyodacite magma. Earth and Planetary Science Letters, 300:246-254

Budd DA, Troll VR, Deegan FM, Jolis EM, Smith VC, Whitehouse MJ, Harris C, Freda C, Hilton DR, Halldórsson SA, Bindeman IN (2017) Magma reservoir dynamics at Toba caldera, Indonesia, recorded by oxygen isotope zoning in quartz. Scientific Reports, 7:40624

Cheng L, Costa F, Carniel R (2017) Unraveling the presence of multiple plagioclase populations and identification of representative two-dimensional sections using a statistical and numerical approach. American Mineralogist, 102:1894-1905

Clynne MA (1999) A complex magma mixing origin for multiple volcanic lithologies erupted in 1915 from Lassen Peak, California. Journal of Petrology, 40:105-132

Cooper KM, Kent AJR (2014) Rapid remobilization of magmatic crystals kept in cold storage. Nature, 506:480-483

Cooper KM, Reid MR (2003) Re-examination of crystal ages in recent Mount St. Helens lavas: implications for magma reservoir processes. Earth and Planetary Science Letters, 213:149-167

Costa F, Chakraborty S, Dohmen R (2003) Diffusion coupling between trace and major elements and a model for calculation of magma residence times using plagioclase. Geochimica et Cosmochimica, 67:2189-2200

Costa F, Dohmen R, Chakraborty S (2008) Time scales of magmatic processes from modeling the zoning patterns of crystals. Reviews in Mineralogy and Geochemistry, 69:545-594

Always consult and cite the final, published document. See http:/www.minsocam.org or GeoscienceWorld

This is the peer-reviewed, final accepted version for American Mineralogist, published by the Mineralogical Society of America.
The published version is subject to change. Cite as Authors (Year) Title. American Mineralogist, in press.
DOI: https://doi.org/10.2138/am-2021-7491. http://www.minsocam.org/

Couch S, Sparks R, Carroll M (2003) The kinetics of degassing-induced crystallization at Soufriere Hills Volcano, Montserrat. Journal of Petrology, 44:1477-1502

Davidson JP, Tepley FJ III (1997) Recharge in volcanic systems;evidence from isotope profiles of phenocrysts. Science, 275: 826–829

Davidson J, Tepley F III, Palacz Z, Meffan-Main S (2001) Magma recharge, contamination and residence times revealed by in situ laser ablation isotopic analysis of feldspar in volcanic rocks. Earth and Planetary Science Letters, 184: 427–442

DeGruyter W, Huber C (2014) A model for eruption frequency of upper crustal silicic magma chambers. Earth and Planetary Science Letters, 403: 117-130

Donaldson CH (1985) The rates of dissolution of olivine, plagioclase, and quartz in a basalt melt. Mineralogical Magazine, 49:683-693

Eichelberger JC (1978) Andesitic volcanism and crustal evolution. Nature, 275: 21–27

Espindola JM, Macias JL, Tilling RI, Sheridan MF (2000) Volcanic history of El Chichón Volcano (Chiapas, Mexico) during the Holocene, and its impact on human activity. Bulletin of Volcanology, 62:90-104

Gardner JE, Rutherford MJ, Carey S, Sigurdsson H (1995) Experimental constraints on pre-eruptive water contents and changing magmatic storage conditions prior to explosive eruptions of Mount St. Helens volcano. Bulletin of Volcanology, 57:1-17

Gerlach DC, Grove TL (1982) Petrology of Medicine Lake Highland Volcanics: Characterization of endmembers of magma mixing. Contributions to Mineralogy and Petrology, 80:147-159

Ghiorso MS, Gualda GAR (2015) An H2O-CO2 mixed fluid saturation model compatible with rhyolite-MELTS. Contributions to Mineralogy and Petrology, 169:53

Always consult and cite the final, published document. See http:/www.minsocam.org or GeoscienceWorld

This is the peer-reviewed, final accepted version for American Mineralogist, published by the Mineralogical Society of America.
The published version is subject to change. Cite as Authors (Year) Title. American Mineralogist, in press.
DOI: https://doi.org/10.2138/am-2021-7491. http://www.minsocam.org/

Ghiorso MS, Sack RO (1995) Chemical mass transfer in magmatic processes. IV. A revised and internally consistent thermodynamic model for the interpolation and extrapolation of liquid-solid equilibria in magmatic systems at elevated temperatures and pressures. Contributions to Mineralogy and Petrology, 119:197-212

Gorokhova NV, Melnik OE, Plechov PYu, Shcherbakov VD (2013) Numerical simulation of plagioclase rim growth during magma ascent at Bezimianny Volcano, Kamchatka. Journal of Volcanology and Geothermal Research, 263:172-181

Gualda GAR, Ghiorso MS, Lemons RV, Carley TL (2012) Rhyolite-MELTS: A modified calibration of MELTS optimized for silica-rich, fluid-bearing magmatic systems. Journal of Petrology, 53, 875-890

Haase CS, Chadam J, Feinn D, Ortoleva P (1980) Oscillatory zoning in plagioclase feldspar. Science, 209:272-274

Hammer JE (2004) Crystal nucleation in hydrous rhyolite: Experimental data applied to classical theory. American Mineralogist, 89(11-12):1673-1679

Hammer JE, Rutherford MJ (2002) An experimental study of the kinetics of decompression-induced crystallization in silicic melt. Journal of Geophysical Research, 107(B1):ECV-8-1 doi:10.1029/2001JB000281

Housh TB, Luhr JF (1991) Plagioclase-melt equilibria in hydrous systems. American Mineralogist, 76:477-492

Humphreys M, Blundy JD, Sparks RSJ (2006) Magma evolution and open-system processes at Shiveluch Volcano: Insights from phenocryst zoning. Journal of Petrology, 47:2303-2334

Huppert H, Woods A (2002) The role of volatiles in magma chamber dynamics. Nature, 420: 493-495

Always consult and cite the final, published document. See http:/www.minsocam.org or GeoscienceWorld

This is the peer-reviewed, final accepted version for American Mineralogist, published by the Mineralogical Society of America.
The published version is subject to change. Cite as Authors (Year) Title. American Mineralogist, in press.
DOI: https://doi.org/10.2138/am-2021-7491. http://www.minsocam.org/

Kawamoto T (1992) Dusty and honeycomb plagioclase: indicators of processes in the Uchino stratified magma chamber, Izu Peninsula, Japan. Journal of Volcanology and Geothermal Research, 49:191-208

L'Heureux I, Fowler AD (1994) A nonlinear dynamical model of oscillatory zoning in plagioclase. American Mineralogist, 79:885-891

Lange RA, Frey HM, Hector J (2009) A thermodynamic model for the plagioclase-liquid hygrometer/thermometer. American Mineralogist, 94:494-506

Larsen JF (2005) Experimental study of plagioclase rim growth around anorthite seed crystals in rhyodacite melt. American Mineralogist, 90:417-427

Macias JL, Arce JL, Mora JC, Espindola JM, Saucedo R, Manetti P (2003) A 550-year-old Plinian eruption at El Chichón Volcano, Chiapas, Mexico: Explosive volcanism linked to reheating of the magma reservoir. Journal of Geophysical Research, 108(B12), 2569, doi:10.1029/2003JB002551

Martel C, Pichavant M, Holtz F, Scaillet B, Bourdier J-L, Traineau H (1999) Effects of fO2 and H2O on andesite phase relations between 2 and 4 kbar. J Geophys Res 104:29453-29470

Mollard E, Martel C, Bourdier J-L (2012) Decompression-induced crystallization in hydrated silica-rich melts: empirical models of experimental plagioclase nucleation and growth kinetics. Journal of Petrology, 53(8):1743-1766

Nelson ST, Montana A (1992) Sieve-textured plagioclase in volcanic rocks produced by rapid decompression. American Mineralogist, 77: 1242–1249.

Putirka K (2005) Igneous thermometers and barometers based on plagioclase+liquid equilibria: tests of some existing models and new calibrations. American Mineralogist, 90:336-346

Always consult and cite the final, published document. See http:/www.minsocam.org or GeoscienceWorld

This is the peer-reviewed, final accepted version for American Mineralogist, published by the Mineralogical Society of America.
The published version is subject to change. Cite as Authors (Year) Title. American Mineralogist, in press.
DOI: https://doi.org/10.2138/am-2021-7491. http://www.minsocam.org/

Rutherford MJ, Sigurdsson H, Carey S, Davis A (1985) The May 18, 1980, eruption of Mount St. Helens 1. Melt composition and experimental phase equilibria. Journal of Geophysical Research, 90:2929-2947

Salisbury MJ, Bohrson WA, Clynne MA, Ramos FC, Hoskin P (2008) Multiple plagioclase crystal populations identified by crystal size distributions and in situ chemical data: Implications for timescales of magma chamber processes associated with the 1915 eruption of Lassen Peak, CA. Journal of Petrology, 49: 1755-1780

Segall P (2016) Repressurization following eruption from a magma chamber with a viscoelastic aureole. Journal of Geophysical Research, 121:8501-8522

Shea T, Hammer JE (2013) Kinetics of cooling-and decompression-induced crystallization in hydrous mafic-intermediate magmas. J Volcanol Geotherm Res 260:127-145

Shea T, Hammer JE, Hellebrand E, Mourey AJ, Costa F, First EC, Lynn KJ, Melnik O (2019) Phosphorous and aluminum zoning in olivine: contrasting behavior of two nominally incompatible elements. Contributions to Mineralogy and Petrology, 174:85

Singer BS, Dungan MA, Layne GD (1995) Textures and Sr, Ba, Mg, Fe, K and Ti compositional profiles in volcanic plagioclase: Clues to the dynamics of calc-alkaline magma chambers: American Mineralogist, 80: 776–798.

Sosa-Ceballos G, Gardner JE, Lassiter JC (2014) Intermittent mixing processes occurring before Plinian eruptions of Popocateptl volcano, Mexico: insights from textural-compositional variations in plagioclase and Sr-Nd-Pb isotopes. Contributions to Mineralogy and Petrology, 167:966

Always consult and cite the final, published document. See http:/www.minsocam.org or GeoscienceWorld

Streck MJ, Broderick CA, Thornber CR, Clynne MA, Pallister JS (2008) Plagioclase populations and zoning in dacite of the 2004-2005 Mount St. Helens eruption; constraints form magma origin and dyanmics. U S Geological Survey Professional Paper 1750: 791-808

Szramek L, Gardner JE, Larsen J (2006) Degassing and microlite crystallization of basaltic andesite magma erupting at Arenal Volcano, Costa Rica. Journal of Volcanology and Geothermal Research, 157: 182-201

Tepley FJ III, Davidson JP, Clynne MA (1999) Magmatic interactions as recorded in plagioclase phenocrysts of Chaos Crags, Lassen volcanic center, California. Journal of Petrology, 40:787-806

Tepley FJ III, Davidson JP, Tilling RI, Arth JG (2000) Magma mixing, recharge and eruption histories recorded in plagioclase phenocrysts from El Chichón Volcano, Mexico. Journal of Petrology, 41:1397-1411

Townsend M, Huber C, Degruyter W, Bachmann O (2019) Magma chamber growth during inter-caldera periods; insights from thermo-mechanical modeling with applications to Laguna del Maule, Campi Flegrei, Santorini, and Aso. Geochemistry Geophysics and Geosystems, 20:1574-1591

Tsuchiyama A (1985) Dissolution kinetics of plagioclase in the melt of the system diopside-albite-anorthite, and the origin of dusty plagioclase in andesites. Contributions to Mineralogy and Petrology, 43:243-270

Vance JA (1965) Zoning in igneous plagioclase: Patchy zoning. Journal of Geology, 73: 636–651

Wallace GS, Bergantz GW (2002) Wavelet-based correlation (WBC) of crystal populations and magma mixing. Earth and Planetary Science Letters, 202:133-145

Always consult and cite the final, published document. See http:/www.minsocam.org or GeoscienceWorld

This is the peer-reviewed, final accepted version for American Mineralogist, published by the Mineralogical Society of America.
The published version is subject to change. Cite as Authors (Year) Title. American Mineralogist, in press.
DOI: https://doi.org/10.2138/am-2021-7491. http://www.minsocam.org/

Wallace GS, Bergantz GW (2004) Constraints on mingling crystal populations from off-center zoning profiles: a statistical approach. American Mineralogist, 89:64-73

Wallace GS, Bergantz GW (2005) Reconciling heterogeneity in crystal zoning data: An application of shared characteristic diagrams at Chaos Crags, Lassen Volcanic Center, California. Contributions to Mineralogy and Petrology, 149:98-112

Waters LE, Andrews BJ, Lange RA (2015) Rapid crystallization of plagioclase phenocrysts in silicic melts during fluid-saturated ascent: Phase equilibrium and decompression experiments. Journal of Petrology, 56: 981-1006. doi:10.1093/petrology/egv025.

Waters LE, Lange RA (2015) An updated calibration of the plagioclase-liquid hygrometer-thermometer applicable to basalts through rhyolites. American Mineralogist, 100:2172-2184

Zhang Y, Xu Z (2016) Zircon saturation and Zr diffusion in rhyolitic melts, and zircon growth speedometer. American Mineralogist, 101:1252-1267

Always consult and cite the final, published document. See http:/www.minsocam.org or GeoscienceWorld

This is the peer-reviewed, final accepted version for American Mineralogist, published by the Mineralogical Society of America.
The published version is subject to change. Cite as Authors (Year) Title. American Mineralogist, in press.
DOI: https://doi.org/10.2138/am-2021-7491. http://www.minsocam.org/

Plagioclase population dynamics and zoning in response to changes in temperature and pressure

Benjamin J. Andrews

Global Volcanism Program, Smithsonian Institution, Washington, DC 20560

For submission to **American Mineralogist**

Figures:

Figure 1. A) BSE image of El Chichón Unit E sample CHI9516 (1465-1520 yBP) plagioclase with line indicating core-to-rim transect. Age from Espindola et al. (2000). B) Core-to-rim transect illustrating variation in An.

Figure 2. Schematic of SNGPlag crystal nucleation, growth, and dissolution. At each time t_i, N_i crystals can nucleate. Over the subsequent time step, those nuclei and all existing crystals grow (or dissolve) depending on supersaturation $\Delta\phi$. To balance long model durations with computational limitations, temporary populations of newly nucleated crystals are tracked (light gray) at high temporal resolution, and then synthesized into a single crystal class (dark gray) with characteristic size and number density N calculated every 120 time steps. Those "through-going" classes continue to grow (or dissolve) throughout the rest of the run. Dissolution can eliminate crystals from the temporary and through-going populations.

Figure 3. Schematic of crystal growth-dissolution cycles, with higher An zones shown in lighter gray. Crystals grow at axis-specific rates proportional to supersaturation $\Delta\phi$, with c->b-

Always consult and cite the final, published document. See http:/www.minsocam.org or GeoscienceWorld

This is the peer-reviewed, final accepted version for American Mineralogist, published by the Mineralogical Society of America.
The published version is subject to change. Cite as Authors (Year) Title. American Mineralogist, in press.
DOI: https://doi.org/10.2138/am-2021-7491. http://www.minsocam.org/

>a-axis rates, resulting in elongate or tabular crystals. Dissolution is assumed to occur at the same rates for all axes, but dissolution along a particular axis stops when a zone of stable An is intersected. Repeated dissolution-growth cycles result in zoned crystals, with some zones dissolved from some or all crystal faces..

Figure 4. A) Variation in supersaturation $\Delta\phi$ with time for rapid heating from T_o=800 °C and cooling from T_o=900 or 1000 °C. The cooling paths (ΔT=100, 150, and 200 °C) follow essentially identical decreases in $\Delta\phi$. The heating paths show similar functional forms, but are offset by the differences between their initial $\Delta\phi$. B) Changes in the magnitudes of nucleation (I) and growth or dissolution rates (J) affect how quickly a magma returns to equilibrium. The rate at which a system returns to equilibrium is proportional to both I and J during crystallization, but mostly dependent upon J during dissolution.

Figure 5. 2-year SNGPlag run with no volume addition at P=100 MPa. A) Temperature-time series. B) Equilibrium ($\phi_{EQBplag}$) and calculated (ϕ_{plag}) plagioclase crystal fractions and supersaturation ($\Delta\phi$). C) Survival diagram indicating crystal nucleation and residence time in the magma. D) Plagioclase number density N_v. E) Characteristic crystal size Sn and lengths L_a, L_b, L_c. F) Characteristic crystal shape for all crystals ("All") at each time and only those nucleated during the model run ("New"). The upper line indicates the ratio of b- to c-axis length, and the lower line a- to c-axis length; the two lines together thus describe how equant, tabular, or elongate the crystals are. Supplementary Material 3 describes this method of plotting shape.

Figure 6. 2-year SNGPlag run with 0.25 volume fraction addition during each heating event. A) Temperature-time series. B) Equilibrium ($\phi_{EQBplag}$) and calculated (ϕ_{plag}) plagioclase crystal fractions and supersaturation ($\Delta\phi$). C) Survival diagram. D) Plagioclase number

Always consult and cite the final, published document. See http:/www.minsocam.org or GeoscienceWorld

This is the peer-reviewed, final accepted version for American Mineralogist, published by the Mineralogical Society of America.
The published version is subject to change. Cite as Authors (Year) Title. American Mineralogist, in press.
DOI: https://doi.org/10.2138/am-2021-7491. http://www.minsocam.org/

density N_v. E) Characteristic crystal size Sn and lengths L_a, L_b, L_c. F) Characteristic shape for all crystals at each time ("All") and only those nucleated during the model run ("New").

Figure 7. Effects of different volume additions V_{input} during otherwise identical SNGPlag runs with three 60-day 150 °C heating events from T_o=750 °C. With V_{input}=0, only the peak An values from the first two events survive. As V_{input} increases, the three recharge events become more distinct in the crystal record. At V_{input}>0.25, some crystallization from between the recharge events is preserved. The double-peaked structure in the zoning patterns results from MELTS calculating non-monotonic variation in An between 750 and 800 °C at 100 MPa.

Figure 8. Modeled compositional zoning and time intervals recorded by crystals nucleated at t=1 day for the scenarios shown in Figures 6 and 7. Model runs with V_{input}=0 record very little zoning in the a- and b-axes (panels A-D), whereas those with V_{input}=0.25 show well developed zones and virtually no missing time intervals. The c-axis shows zoning in both scenarios, although the zones are highly compressed (E) and have substantial time missing for the V_{input}=0 condition (F).

Figure 9. SNGPlag results for increasing ("Inc.") or decreasing ("Dec.") magnitude heating sequences. A) Temperature-time series. B) Supersaturation $\Delta\phi$. C) Survival diagram. D) Plagioclase number density N_v. E) Characteristic crystal size (Sn) and c-axis length (L_c). F) Characteristic shape for crystals nucleated during the two runs. In all panels, the heavy line represents the increasing series and the thin line the decreasing series.

Always consult and cite the final, published document. See http:/www.minsocam.org or GeoscienceWorld

This is the peer-reviewed, final accepted version for American Mineralogist, published by the Mineralogical Society of America.
The published version is subject to change. Cite as Authors (Year) Title. American Mineralogist, in press.
DOI: https://doi.org/10.2138/am-2021-7491. http://www.minsocam.org/

Figure 10. 2-year SNGPlag run at 800 °C. A) Pressure-time series. B) Equilibrium ($\phi_{EQBplag}$) and calculated (ϕ_{plag}) plagioclase crystal fractions and supersaturation ($\Delta\phi$). C) Survival diagram. D) Plagioclase number density N_v.

Figure 11. A) 5-year temperature-time series used in full and parameterized SNGPlag run. B) Comparison of $\Delta\phi$ for the two runs. Because $\Delta\phi$ controls crystallization and dissolution rates, good agreement between $\Delta\phi$ for the runs shows the parameterized run accurately reproduces the full run crystallization record .

Figure 12. A) Temperature and B) pressure series for the 5269-year run. The run comprises 454 heating events and 12 decompressions or eruptions in 26 groups.

Figure 13. A) C-axis core-to-rim transects during 5269-year time series, and pseudo-back-scattered electron sections through the growing crystal. B) Histogram showing cumulative thickness as a function of composition for the final (5269-year) crystal (bin size of 0.01 An). C) Input and recorded (crystallized) conditions shown as histogram of time. D) Ratio of recorded to input time as a function of pressure-temperature conditions (and thus An).

Table 1. Whole rock composition (in anhydrous wt.%) of El Chichón trachyandesite used as input for MELTS and SNGPlag. Analysis from Macias et al. (2003) and Andrews et al., (2008).

SiO2	TiO2	Al2O3	FeO	MnO	MgO	CaO	Na2O	K2O	P2O5	Total	fO2 ($\log_{10}$)
56.28	0.74	19.34	6.52	0.19	2.47	7.57	2.48	3.92	0.36	99.87	NNO+2.3

Always consult and cite the final, published document. See http:/www.minsocam.org or GeoscienceWorld

This is the peer-reviewed, final accepted version for American Mineralogist, published by the Mineralogical Society of America.
The published version is subject to change. Cite as Authors (Year) Title. American Mineralogist, in press.
DOI: https://doi.org/10.2138/am-2021-7491. http://www.minsocam.org/

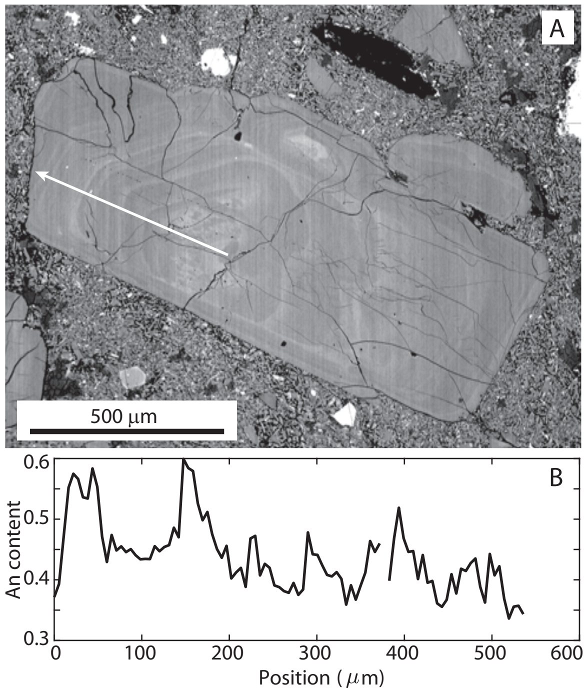

Figure 1

Always consult and cite the final, published document. See http:/www.minsocam.org or GeoscienceWorld

This is the peer-reviewed, final accepted version for American Mineralogist, published by the Mineralogical Society of America.
The published version is subject to change. Cite as Authors (Year) Title. American Mineralogist, in press.
DOI: https://doi.org/10.2138/am-2021-7491. http://www.minsocam.org/

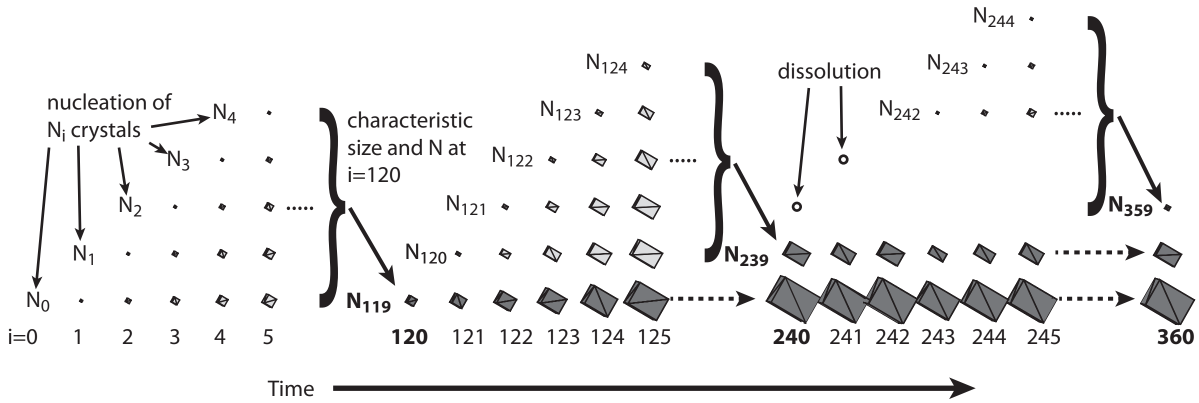

Figure 2

Always consult and cite the final, published document. See http:/www.minsocam.org or GeoscienceWorld

This is the peer-reviewed, final accepted version for American Mineralogist, published by the Mineralogical Society of America.
The published version is subject to change. Cite as Authors (Year) Title. American Mineralogist, in press.
DOI: https://doi.org/10.2138/am-2021-7491. http://www.minsocam.org/

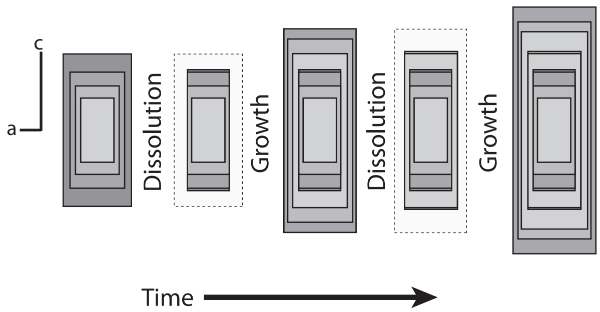

Figure 3

Always consult and cite the final, published document. See http:/www.minsocam.org or GeoscienceWorld

This is the peer-reviewed, final accepted version for American Mineralogist, published by the Mineralogical Society of America.
The published version is subject to change. Cite as Authors (Year) Title. American Mineralogist, in press.
DOI: https://doi.org/10.2138/am-2021-7491. http://www.minsocam.org/

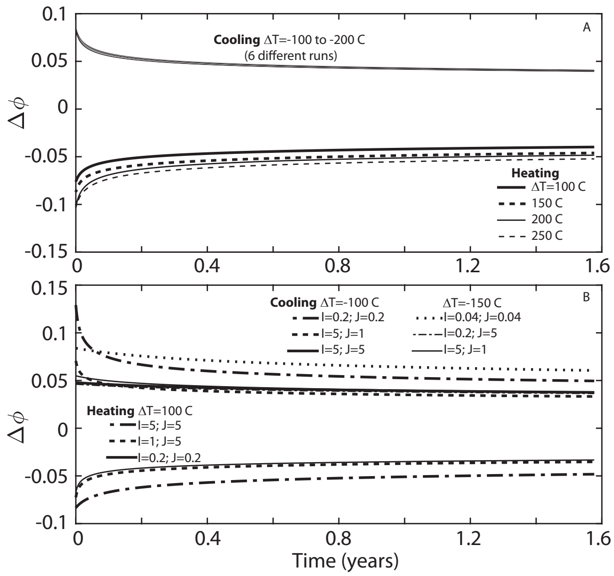

Figure 4

Always consult and cite the final, published document. See http:/www.minsocam.org or GeoscienceWorld

This is the peer-reviewed, final accepted version for American Mineralogist, published by the Mineralogical Society of America.
The published version is subject to change. Cite as Authors (Year) Title. American Mineralogist, in press.
DOI: https://doi.org/10.2138/am-2021-7491. http://www.minsocam.org/

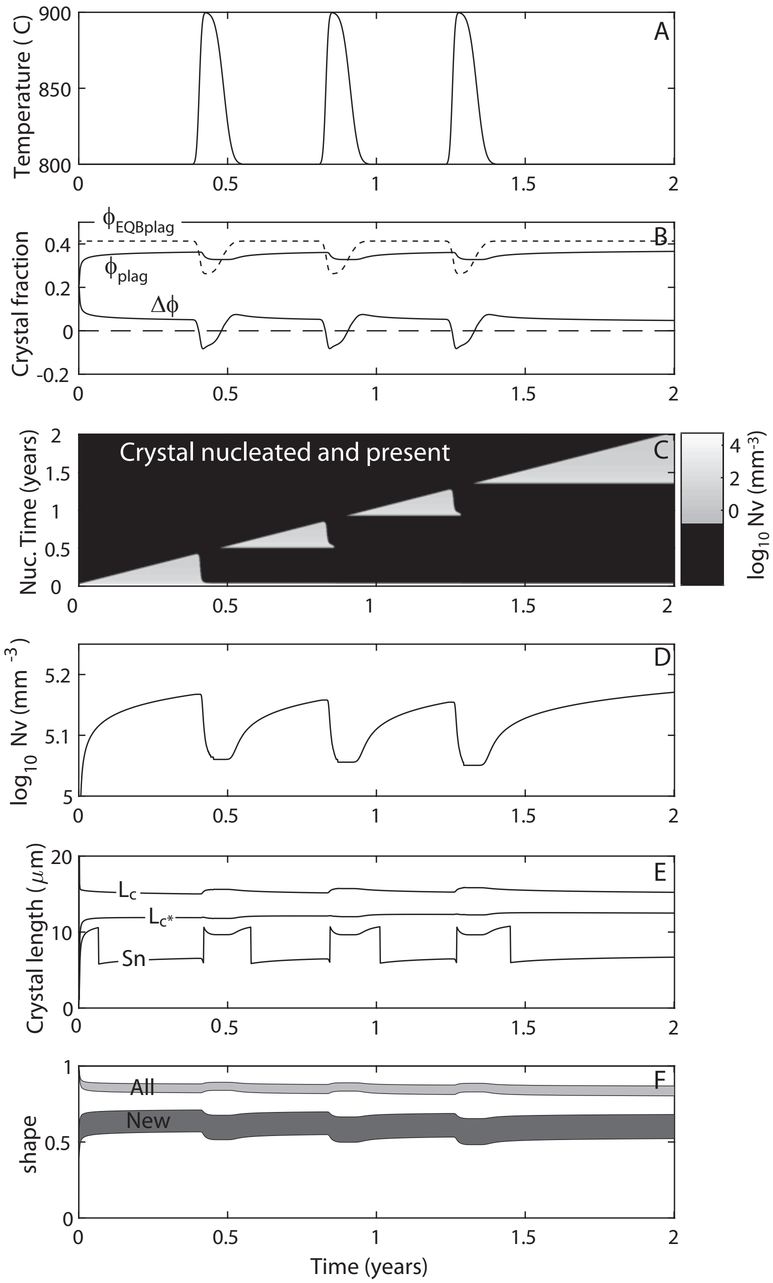

Figure 5

Always consult and cite the final, published document. See http:/www.minsocam.org or GeoscienceWorld

This is the peer-reviewed, final accepted version for American Mineralogist, published by the Mineralogical Society of America.
The published version is subject to change. Cite as Authors (Year) Title. American Mineralogist, in press.
DOI: https://doi.org/10.2138/am-2021-7491. http://www.minsocam.org/

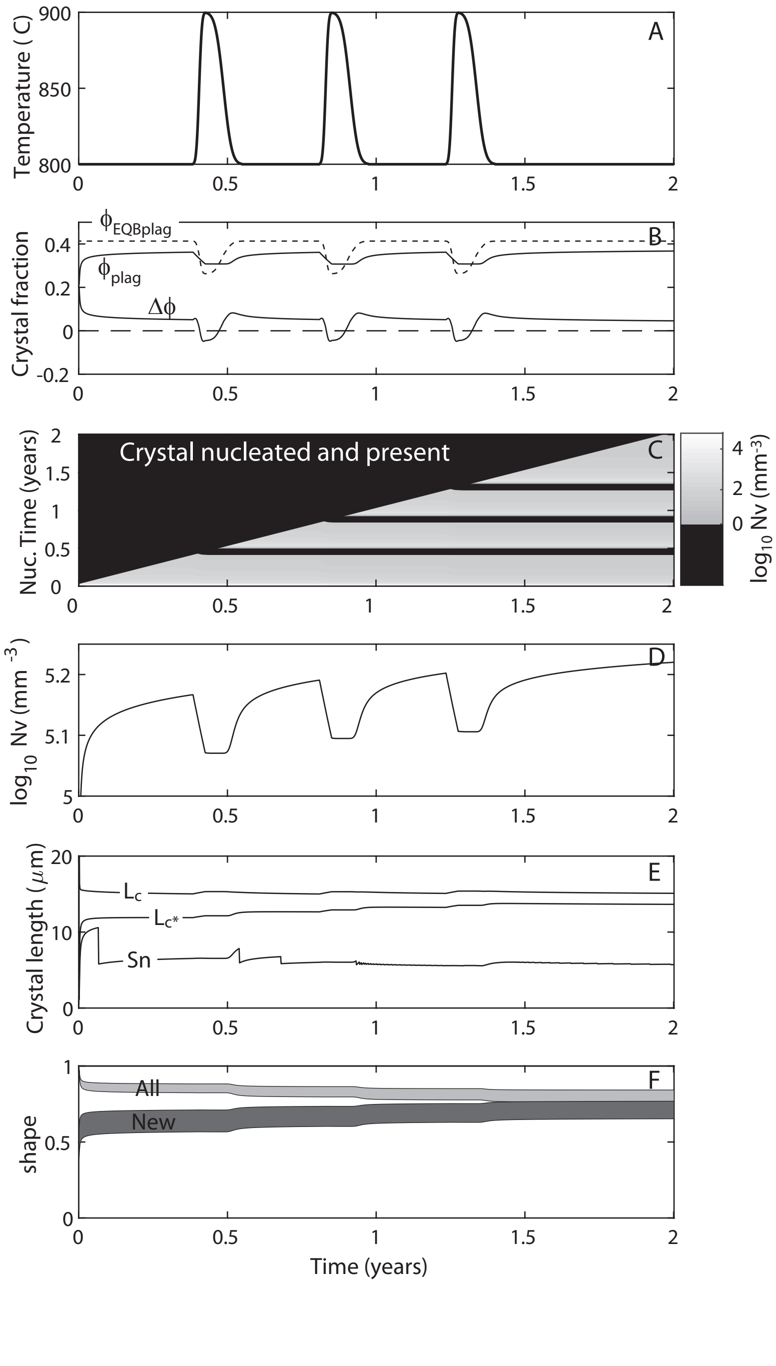

Figure 6

Always consult and cite the final, published document. See http:/www.minsocam.org or GeoscienceWorld

This is the peer-reviewed, final accepted version for American Mineralogist, published by the Mineralogical Society of America.
The published version is subject to change. Cite as Authors (Year) Title. American Mineralogist, in press.
DOI: https://doi.org/10.2138/am-2021-7491. http://www.minsocam.org/

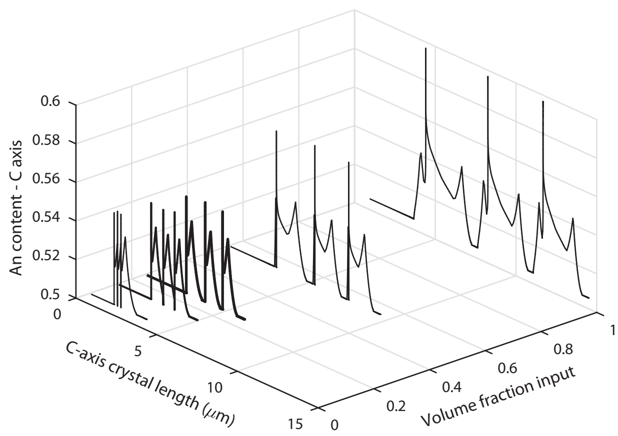

Figure 7

This is the peer-reviewed, final accepted version for American Mineralogist, published by the Mineralogical Society of America.
The published version is subject to change. Cite as Authors (Year) Title. American Mineralogist, in press.
DOI: https://doi.org/10.2138/am-2021-7491. http://www.minsocam.org/

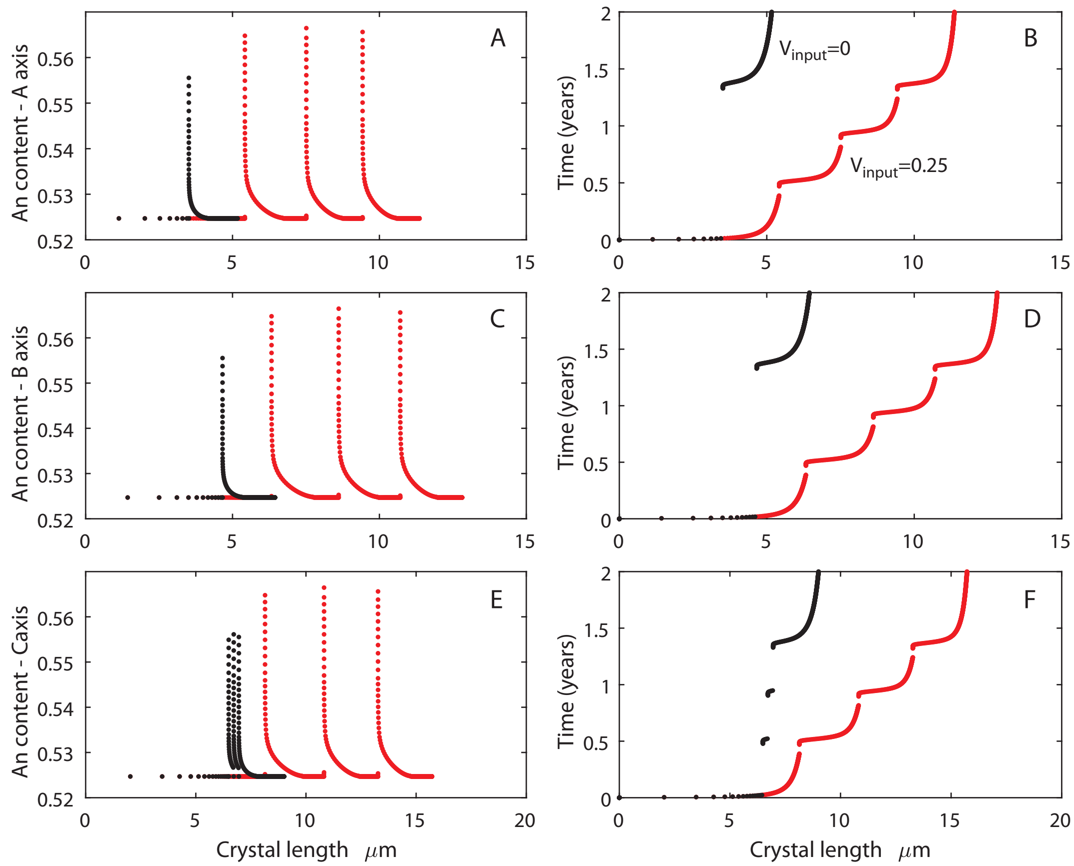

Figure 8

Always consult and cite the final, published document. See http:/www.minsocam.org or GeoscienceWorld

This is the peer-reviewed, final accepted version for American Mineralogist, published by the Mineralogical Society of America.
The published version is subject to change. Cite as Authors (Year) Title. American Mineralogist, in press.
DOI: https://doi.org/10.2138/am-2021-7491. http://www.minsocam.org/

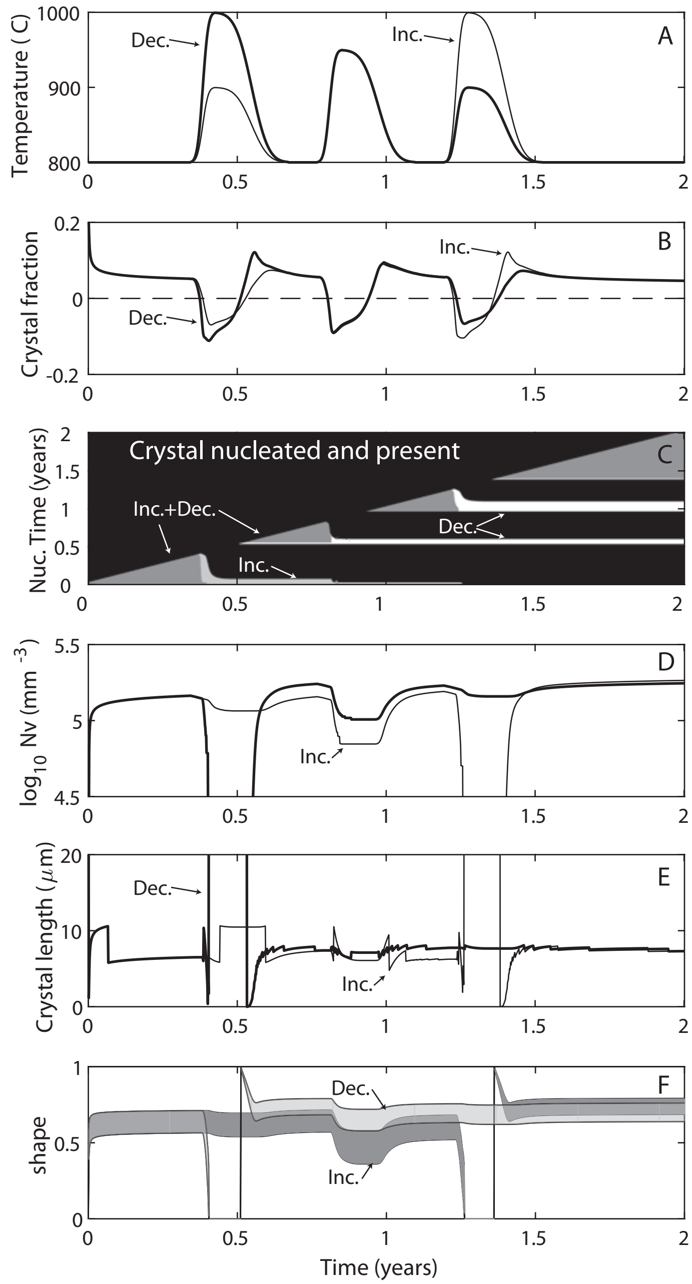

Figure 9

Always consult and cite the final, published document. See http:/www.minsocam.org or GeoscienceWorld

This is the peer-reviewed, final accepted version for American Mineralogist, published by the Mineralogical Society of America.
The published version is subject to change. Cite as Authors (Year) Title. American Mineralogist, in press.
DOI: https://doi.org/10.2138/am-2021-7491. http://www.minsocam.org/

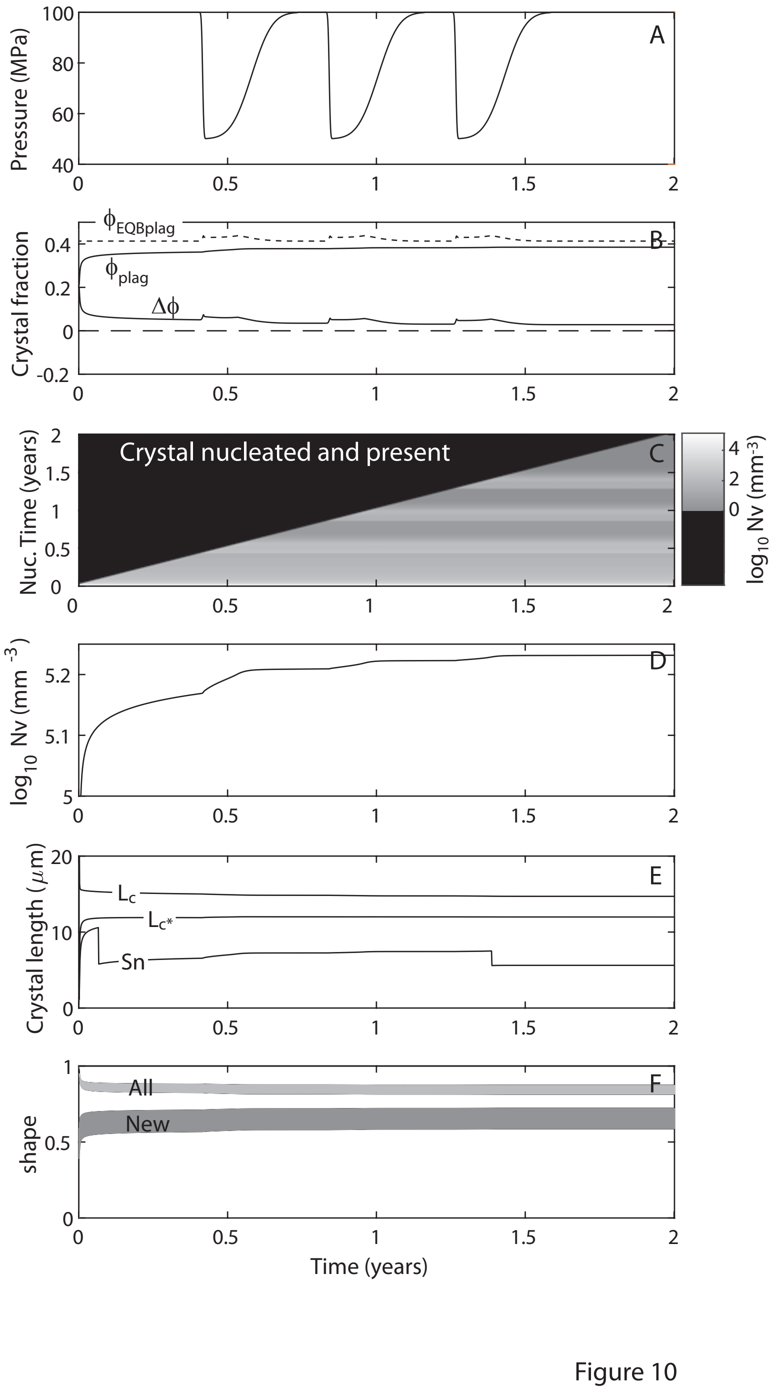

Figure 10

Always consult and cite the final, published document. See http:/www.minsocam.org or GeoscienceWorld

This is the peer-reviewed, final accepted version for American Mineralogist, published by the Mineralogical Society of America.
The published version is subject to change. Cite as Authors (Year) Title. American Mineralogist, in press.
DOI: https://doi.org/10.2138/am-2021-7491. http://www.minsocam.org/

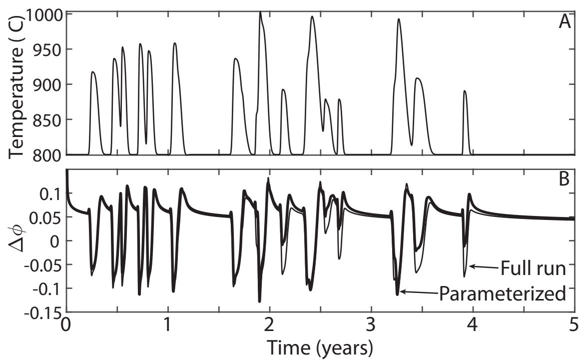

Figure 11

Always consult and cite the final, published document. See http:/www.minsocam.org or GeoscienceWorld

This is the peer-reviewed, final accepted version for American Mineralogist, published by the Mineralogical Society of America.
The published version is subject to change. Cite as Authors (Year) Title. American Mineralogist, in press.
DOI: https://doi.org/10.2138/am-2021-7491. http://www.minsocam.org/

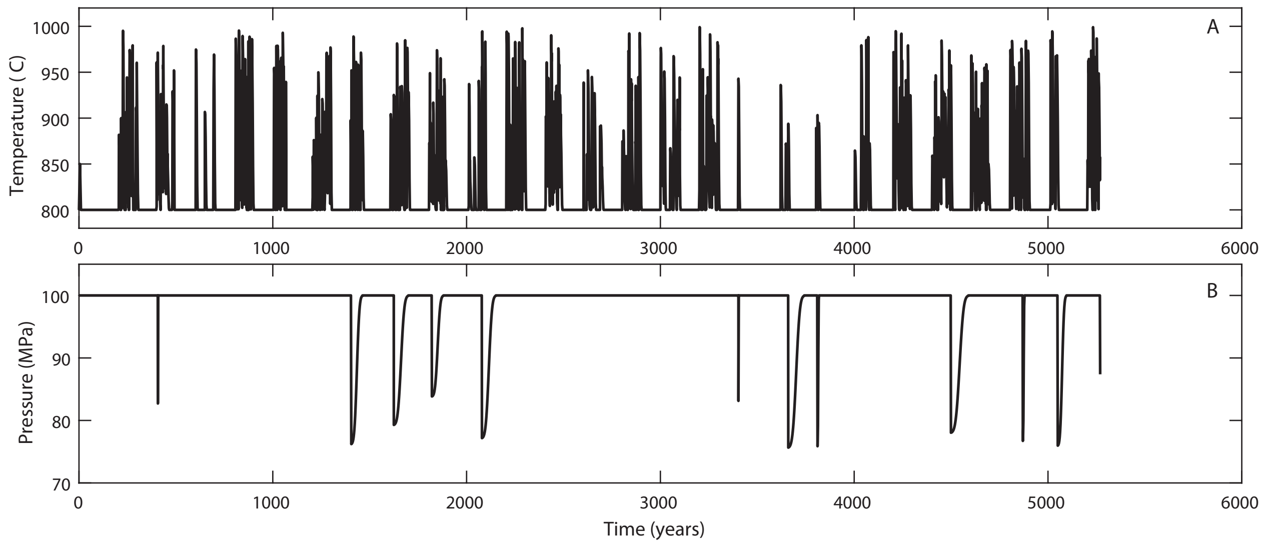

Figure 12

Always consult and cite the final, published document. See http:/www.minsocam.org or GeoscienceWorld

This is the peer-reviewed, final accepted version for American Mineralogist, published by the Mineralogical Society of America.
The published version is subject to change. Cite as Authors (Year) Title. American Mineralogist, in press.
DOI: https://doi.org/10.2138/am-2021-7491. http://www.minsocam.org/

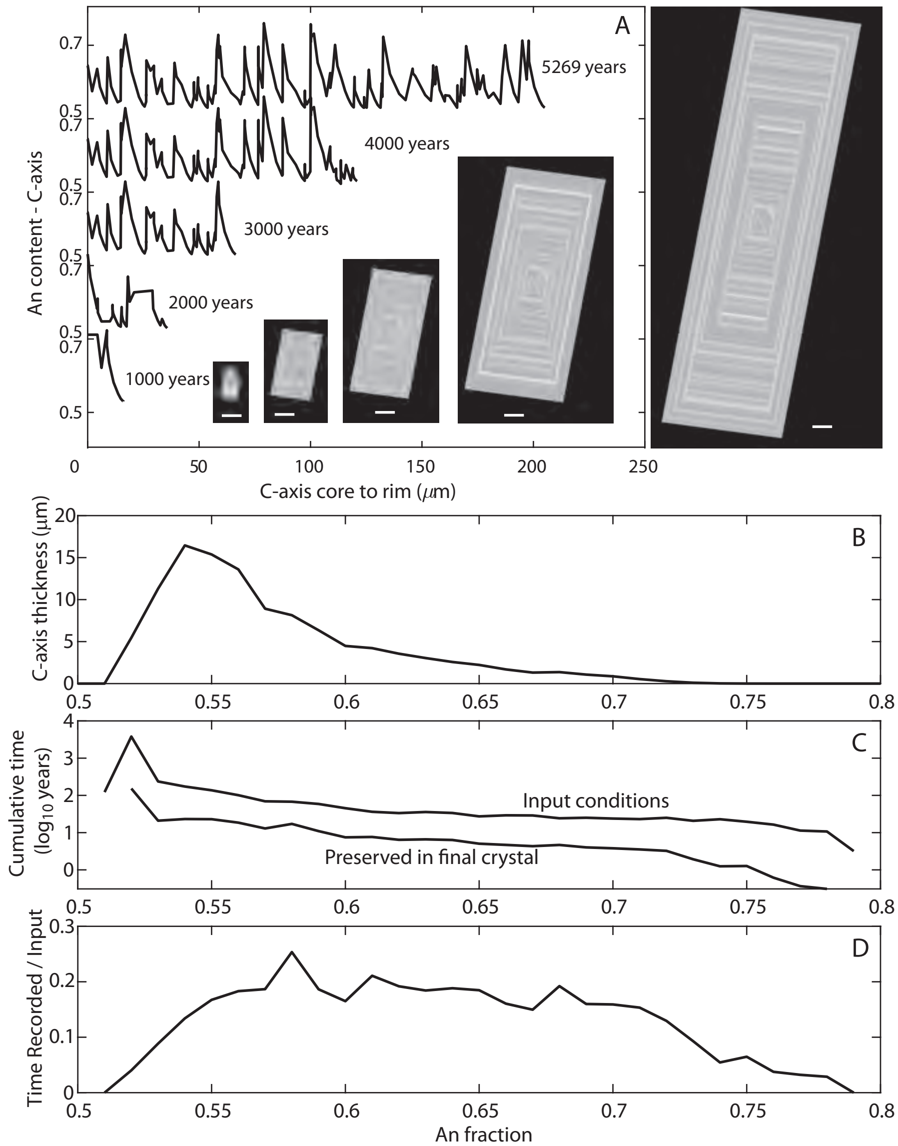

Figure 13

Always consult and cite the final, published document. See http:/www.minsocam.org or GeoscienceWorld